Frontiers in Bioscience Landmark

Front. Biosci. (Landmark Ed) **2025**; 30(3): 26898
https://doi.org/10.31083/FBL26898

Original Research

Transcription Factor FOSL1 Promotes Cisplatin Resistance in Non-Small Cell Lung Cancer Cells by Modulating the Wnt3a/β-Catenin Signaling through Upregulation of PLIN3 Expression

Wanning Tong[1,†], Jianjun Sun[1,†], Bin Shen[1], Yaohua Hu[1], Chenxing Wang[1], Min Rao[1], Jin Li[1], Delin Xia[1], Jiagui Dong[1], Hong Wang[1], Dongmei Zhu[1], Haibo Wu[1,*], Zhigang Cai[1,*]

[1]Department of Respiratory and Critical Care Medicine, PLA Navy Medical Center, 200052 Shanghai, China
*Correspondence: 18964573125@189.com (Haibo Wu); caizg12345@aliyun.com (Zhigang Cai)
[†]These authors contributed equally.

Academic Editor: Amancio Carnero Moya
Submitted: 10 October 2024 Revised: 23 January 2025 Accepted: 30 January 2025 Published: 19 March 2025

Abstract

Background: Lung adenocarcinoma (LUAD) is the most prevalent histological subtype of lung cancer, accounting for 45.3% of all cases and serving as a major cause of cancer-related mortality. Although cisplatin (DDP) is a cornerstone in LUAD therapy, its efficacy is often compromised by resistance, leading to therapeutic failure and poor patient outcomes. Lipid metabolism and associated proteins, such as perilipin 3 (PLIN3), have been increasingly implicated in cancer progression and chemoresistance. However, the precise mechanisms through which PLIN3 contributes to cisplatin (DDP) resistance in LUAD remain poorly understood. **Methods**: To investigate the role of PLIN3 in DDP resistance, its expression in LUAD tissues and its correlation with patient prognosis were analyzed using bioinformatics databases and validated through clinical sample analysis. The effects of *PLIN3* knockdown and overexpression on DDP resistance and Wnt3a/β-catenin signaling were assessed using quantitative real-time PCR (qPCR), western blotting, cytotoxicity assays, and colony formation assays. Bioinformatics screening identified FOS-like antigen 1 (FOSL1) as a transcription factor positively correlated with PLIN3, and its involvement in DDP resistance was further examined both *in vitro* and *in vivo*. **Results**: PLIN3 expression is significantly elevated in LUAD tissues and correlates with poor overall survival. In LUAD cells, PLIN3 overexpression enhanced DDP resistance by upregulating Wnt3a expression and promoting β-catenin nuclear translocation. Bioinformatics analysis identified FOSL1 as a key transcription factor regulating PLIN3 expression. Experimental validation confirmed that FOSL1 directly binds to the PLIN3 promoter, activating the Wnt3a/β-catenin pathway and promoting DDP resistance. Knockdown of PLIN3 or inhibition of Wnt3a signaling reversed the effects of FOSL1 overexpression on DDP resistance. **Conclusion**: This study demonstrates that PLIN3 contributes to DDP resistance in LUAD by activating the Wnt3a/β-catenin signaling pathway, with FOSL1 acting as a critical upstream regulator. Targeting the FOSL1/PLIN3/Wnt/β-catenin axis may provide a promising therapeutic strategy for overcoming chemoresistance in LUAD.

Keywords: lung cancer; chemoresistance; FOSL1; PLIN3; Wnt; β-catenin

1. Introduction

Lung cancer remains the leading cause of cancer incidence and mortality worldwide, accounting for 12.4% of all cancer diagnoses and 18.7% of cancer-related deaths [1]. Non-small cell lung cancer (NSCLC) represents the predominant subtype, encompassing lung adenocarcinoma (LUAD), lung squamous cell carcinoma (LUSC), and large cell carcinoma (LCC) [2]. Among these, LUAD is the most prevalent, constituting approximately 45.3% of all lung cancers, exceeding the incidence of LUSC at 20.1% and LCC at 7.4% [2].

Cisplatin (DDP) remains a cornerstone of chemotherapy for NSCLC due to its broad-spectrum anti-tumor activity [3,4]. However, the development of DDP resistance presents a significant barrier to its clinical efficacy [5,6]. Evidence reveals substantial variability in DDP sensitivity across different NSCLC subtypes [7,8], with LUAD exhibiting a higher degree of resistance compared to LUSC, potentially due to differences in inflammatory responses and the tumor microenvironment [7,8]. Therefore, understanding the mechanisms driving DDP resistance in LUAD is critical for improving therapeutic outcomes.

Lipid metabolism reprogramming is a hallmark of cancer, facilitating rapid tumor cell proliferation and survival by modulating fatty acid synthesis, oxidation, and storage [9–12]. This metabolic adaptability not only provides energy and essential components for tumor cells but may also contribute to their resistance to chemotherapy, thereby promoting drug resistance [9–12]. For example, lipid metabolism in LUAD regulates osimertinib resistance *via* the epidermal growth factor receptor (EGFR) signaling pathway [13].

Lipid droplets (LDs) play a central role in lipid metabolism, with their dynamic regulation responsive to

cellular lipid and energy demands [14–16]. Perilipin 3 (PLIN3), a member of the perilipin protein family, regulates LD formation and lipid storage [17]. Recent studies have highlighted PLIN3's association with tumor progression, increased invasiveness, and poor prognosis in various cancers [18–21]. In lung cancer, PLIN3 is significantly upregulated in early-stage tissues, indicating the critical role of LDs in tumor development [22]. Furthermore, PLIN3 has been shown to exert an immune-resistant effect in LUAD, where its silencing reduces Programmed Cell Death Ligand 1 (PD-L1) expression, thereby inhibiting immune evasion and suppressing tumor growth [23].

Although research directly linking PLIN3 to chemotherapy resistance is limited, evidence from other cancers suggests that PLIN3 may modulate chemoresistance through metabolic pathways, including autophagy. For instance, inhibition of PLIN3 in prostate cancer enhances autophagic activity and promotes resistance to docetaxel, while Perilipin 4 (PLIN4), another member of the perilipin family, has been associated with chemoresistance in triple-negative breast cancer [9,24].

This study investigated the role of PLIN3 in DDP resistance in LUAD. Our results demonstrate that PLIN3 expression is significantly elevated in LUAD and strongly correlates with poor prognosis. Mechanistic studies reveal that PLIN3 promotes DDP resistance by activating the Wnt3a/β-catenin signaling pathway. Further analysis identified FOS-like antigen 1 (FOSL1) as a key transcription factor regulating PLIN3 expression and contributing to DDP resistance. These findings elucidate the critical role of PLIN3 in LUAD and suggest potential molecular targets to enhance the efficacy of DDP treatment.

2. Materials and Methods

2.1 The Cancer Genome Atlas (TCGA) Database and Kaplan-Meier Plotter Database Analysis

The TCGA database was utilized to examine the expression levels of *PLIN3* and its prognostic significance in LUAD (Kaplan-Meier Plotter). RNA-seq data and corresponding clinical information for patients with LUAD were retrieved from the TCGA database *via* the UALCAN portal (https://ualcan.path.uab.edu/). On the UALCAN analysis page (https://ualcan.path.uab.edu/analysis.html), *PLIN3* expression was assessed in LUAD based on sample types, cancer stages, smoking habits, nodal metastasis status, *TP53* mutation status, and histological subtypes. Survival analysis was conducted using both the TCGA and Kaplan-Meier Plotter databases (https://kmplot.com/analysis/). Patients were categorized into two groups based on the median *PLIN3* expression level in LUAD. Survival curves were generated to evaluate the prognostic impact of PLIN3 expression on patient survival. The analysis was performed using the following parameters: Affy ID:202122_s_at; Survival: Overall Survival (OS); Split patients by: median; Follow up threshold: all; Censor at threshold: checked; Compute median over entire database: false; Cutoff value used in analysis: 962; Expression range of the probe: 38-7829; Probe set option: user-selected probe set; Invert HR values below 1: not checked.

Table 1. Clinical characteristics of the included patients.

Characteristics	Cases (24 in total)	Percentage (%)
Sex		
Male (n)	13	54.2%
Female (n)	11	45.8%
Smoking status		
Current smoker	9	37.5%
Ex smoker	7	29.2%
Never smoker	8	33.3%
Age (years)		
<medium (58)	10	41.7%
≥medium (58)	14	58.3%
N classification		
N_0	8	33.3%
N_1	5	20.8%
N_2	6	25.0%
N_3	5	20.9%
Clinical stage		
Stage I	7	29.2%
Stage II	5	20.9%
Stage III	8	33.3%
Stage IV	4	16.6%
Primary tumor size		
Tumor size <3 cm	10	41.7%
Tumor size ≥3 cm	14	58.3%

2.2 Clinical Sample Collection

Tumor and adjacent non-tumor tissue samples were collected from 24 patients with LUAD at the PLA Naval Medical Center (Shanghai, China), with the non-tumor tissues being situated more than 5 cm from the tumor. Only patients with primary LUAD who had not received any prior treatment, including chemotherapy, were included in the study. All tissues were diagnosed histopathologically and clinically. The study was approved by the Ethics Committee of the Naval Medical Center (ethical approval number: AF-HEC-068), and all patients or their families/legal guardians provided written informed consent. The clinical characteristics of the included patients were summarized in Table 1.

2.3 Cell Culture and Transfection

The NSCLC cell lines H2030 (ATCC), H2405, H1755, H2347, H1703, and the lung epithelial cell line BEAS-2B were sourced from American Type Culture Collection (ATCC, Manassas, MD, USA) and cultured in a humidified incubator at 37 °C with 5% CO_2. Cells were maintained in RPMI-1640 medium (Sigma-Aldrich, Shanghai, China) supplemented with 10% fetal bovine serum (FBS,

Sigma-Aldrich, Shanghai, China). All cell lines were validated by short tandem repeat (STR) profiling and tested negative for mycoplasma.

For transfection experiments, cells were seeded in 6-well plates (Sigma-Aldrich, Shanghai, China) at a density of 2×10^5 cells per well and allowed to adhere overnight. Transfection of short hairpin RNA (shRNA), small interfering RNA (siRNA), or overexpression plasmids was performed using Lipofectamine 2000 reagent (Thermo Fisher Scientific, Waltham, MA, USA). Specifically, shRNA transfection utilized a plasmid encoding the shRNA sequence, while siRNA transfection involved specific siRNA sequences targeting the genes of interest. The transfection complexes were prepared in Opti-MEM medium (Thermo Fisher Scientific, Waltham, MA, USA) and applied to the cells for 48–72 hours, after which a fresh complete medium was added. The target sequences used were: si-FOSL1-1: GACTGACAAACTGGAAGATGAGA (349–371); si-FOSL1-2: TACAAACCTACCAAAATGGAATA (1383–1405); si-PLIN3: GGGAAGCTAAGGCTCTCAAAACG (1505–1527).

2.4 Establishment of DDP-Resistant LUAD Cell Lines

The DDP-resistant LUAD cell line was established through gradual drug selection. Parental H2030 and H1775 cells were initially exposed to low concentrations of DDP (0.5–1.0 µg/mL, Sigma-Aldrich, Shanghai, China) and allowed to proliferate until stable growth was observed. The DDP concentration was then incrementally increased by 0.5–1.0 µg/mL every 2–4 weeks, enabling the cells to adapt to each new concentration. This process continued until the cells were able to proliferate stably in high concentrations of DDP (up to 10 µg/mL). Resistance development was confirmed by comparing the half-maximal inhibitory concentration (IC_{50}) of DDP between resistant and parental cells *via* cell viability assays. The resistant cell line was further stabilized by culturing in a DDP-free medium for several passages.

2.5 Quantitative Real-Time PCR (qPCR)

Total RNA was extracted from the cultured cells following the TRIzol reagent protocol (Invitrogen, Thermo Fisher Scientific, Waltham, MA, USA). RNA quality and concentration were assessed using a NanoDrop spectrophotometer (Thermo Fisher Scientific, Waltham, MA, USA). For cDNA synthesis, 1 µg of total RNA was reverse-transcribed using Superscript II Reverse Transcriptase (Thermo Fisher Scientific, Inc., Waltham, MA, USA). QPCR was performed with SYBR Green Master Mix (Thermo Fisher Scientific, Waltham, MA, USA) on a real-time PCR detection system, employing primers specific to the target genes. Glyceraldehyde-3-phosphate dehydrogenase (*GAPDH*) was used as the internal reference for normalization. Negative controls, including no-template controls, were included to exclude contamination or non-specific amplification. Relative expression levels were calculated using the $2^{-\Delta\Delta Ct}$ method. The primers for *FOSL1* were: left primer: AGCTGCAGAAGCAGAAGGAG; right primer: GGAGTTAGGGAGGGTGTGGT. The primers for *PLIN3* were: left primer: CAGCAGAGAAGGGAGTGAGG; right primer: ACACAAGCTCCTTGGTGTCC.

2.6 Western Blot Analysis

Cell lysates were prepared using Radio-Immunoprecipitation Assay (RIPA) buffer (Sigma-Aldrich, Shanghai, China), supplemented with protease and phosphatase inhibitors (Sigma-Aldrich, Shanghai, China). After lysis, the samples were centrifuged at 12,000 rpm for 10 minutes at 4 °C, and the supernatants were collected. Protein concentration was quantified using a bicinchoninic acid (BCA) protein assay kit (Sigma-Aldrich, Shanghai, China). Equal amounts of protein (20–30 µg) were separated by sodium dodecyl sulfate-polyacrylamide gel electrophoresis (SDS-PAGE, Bio-Rad, Shanghai, China) and transferred to Polyvinylidene fluoride (PVDF) membranes (Bio-Rad, Shanghai, China). The membranes were blocked for 1 hour at room temperature with 5% non-fat dry milk in tris-buffered saline with tween (TBST) (Sigma-Aldrich, Shanghai, China), followed by overnight incubation at 4 °C with primary antibodies (anti-PLIN3, SAB1406951, 1 µg/Ml, Sigma-aldrich, Shanghai, China; anti-Wnt3a, ab219412, 1:1000, Abcam, Shanghai, China; anti-β-Catenin, #9582, 1:1000, Cell Signaling Technology, Shanghai, China; anti-Lamin A/C, L1293, 1:1000, Sigma-aldrich, Shanghai, China; anti-FOSL1, SAB1411459, 1 µg/mL, Sigma-aldrich, Shanghai, China; anti-GAPDH, AB2302, 1:10,000, Sigma-aldrich, Shanghai, China). After three washes with TBST, the membranes were incubated with horseradish peroxidase (HRP)-conjugated secondary antibody (Rabbit Anti-Goat lgG Antibody HRP conjugate, AP106P, 1:5,000, Sigma-aldrich, Shanghai, China) for 1.5 hours at room temperature. Protein bands were visualized using an enhanced chemiluminescence (ECL) detection system (Thermo Fisher Scientific, Waltham, MA, USA). Relative protein expression was quantified using ImageJ software (Version 1.53, NIH, Bethesda MD, USA), with GAPDH or Lamin A/C as loading controls. The original Western blot is provided as **Supplementary Material**.

2.7 Cytotoxicity and Cell Viability Assays

The cytotoxicity and cell viability effects of DDP were assessed using the Cell Counting Kit-8 (CCK-8) assay (Sigma-Aldrich, Shanghai, China). Cells were seeded in 96-well plates at a density of 5000 cells per well and incubated overnight to allow attachment. For the cytotoxicity assessment, cells were treated with increasing concentrations of DDP for 48 hours. Following the designated treatment or growth periods (24, 48, or 72 hours), 10 µL of CCK-8 reagent was added to each well, and the plates

were incubated at 37 °C for 2 hours in the dark. Absorbance at 450 nm was measured using a microplate reader (Tecan-UK, Reading, UK), with background correction performed by subtracting the absorbance of wells containing only media and CCK-8. Cell viability or cytotoxicity was calculated as a percentage relative to control cells, with the control group set to 100% for normalization. The half maximal inhibitory concentration (IC_{50}) of DDP was determined by plotting dose-response curves and performing nonlinear regression to identify the concentration required to inhibit 50% of cell viability.

2.8 Colony Formation Assay

For colony formation assays, cells were plated in 6-well plates at a density of 500 cells per well and cultured at 37 °C with 5% CO_2 for 10–14 days to allow colony formation. At the end of the incubation, the culture medium was discarded, and colonies were fixed with 4% paraformaldehyde (Sigma-Aldrich, Shanghai, China) for 15 minutes at room temperature. After fixation, colonies were stained with 0.5% crystal violet (Sigma-Aldrich, Shanghai, China) for 20 minutes and washed with distilled water to remove excess stain. Colonies containing more than 50 cells were counted under a microscope (OLYMPUS IX71, Olympus, Tokyo, Japan), and colony formation efficiency was calculated by dividing the number of colonies formed by the initial cell number.

2.9 Chromatin Immunoprecipitation (CHIP) Assay

Cells were cross-linked with 1% formaldehyde (Sigma-Aldrich, Shanghai, China) for 10 minutes at room temperature to preserve protein-DNA interactions. The reaction was subsequently quenched with 125 mM glycine (Sigma-Aldrich, Shanghai, China). Following this, cells were lysed in chromatin immunoprecipitation (ChIP) lysis buffer (Thermo Fisher Scientific, Waltham, MA, USA), and chromatin was fragmented to an average size of 200–1000 bp by sonication. The sheared chromatin was subjected to overnight immunoprecipitation at 4 °C using antibodies (Anti-FOSL1, ab252421, 1/30, Abcam, Shanghai, China; IgG, I8140, 1/30, Sigma-aldrich, Shanghai, China) specific to the protein of interest or control immunoglobulin G (IgG). Immunoprecipitated DNA-protein complexes were then eluted, and cross-links were reversed by heating at 65 °C for 4 hours. Purified DNA was analyzed by qPCR using primers specific to the target DNA sequences to identify the presence of these sequences in the immunoprecipitates. Results were normalized to input DNA to account for variations in chromatin preparation and PCR efficiency.

2.10 Luciferase Reporter Assay

For luciferase assays, cells were co-transfected with a luciferase reporter plasmid containing the PLIN3 promoter region and a Renilla luciferase plasmid as an internal control to assess transfection efficiency. Forty-eight hours post-transfection, cell lysates were prepared using passive lysis buffer according to the manufacturer's instructions. Luciferase activity was measured using a dual-luciferase reporter assay system (Thermo Fisher Scientific, Waltham, MA, USA), with the firefly luciferase signal, reflecting the promoter activity of the target gene, normalized to the Renilla luciferase signal to correct for transfection efficiency. Relative promoter activity was determined by calculating the ratio of firefly to Renilla luciferase activity.

2.11 Xenograft Tumor Assay

Six-week-old female nude mice (Bikai Keyi Biotechnology Co., Ltd., Shanghai, China) were subcutaneously injected with H2030/DDP cells into the right flank under anesthesia with ketamine (100 mg/mL) and acepromazine (10 mg/mL) at a dose of 100 mg/kg and 5.0 mg/kg, respectively, via intraperitoneal injection. The injected cells had undergone *FOSL1* knockdown, or *FOSL1* knockdown combined with overexpression of *PLIN3* or *Wnt3a*. Mice received intraperitoneal injections of DDP at a dose of 2 mg/kg, twice weekly. Tumor dimensions were measured weekly, and tumor volume was calculated using the formula (length $\times$ width^2)/2 to ensure consistent and accurate measurements. At the study's conclusion, mice were humanely euthanized *via* quick cervical dislocation, and tumors were carefully excised and weighed to evaluate tumor burden. The study adhered to the Animal Research: Reporting of *In Vivo* Experiments (ARRIVE) guidelines 2019 and was approved by the ethical committee of PLA Naval Medical Center.

2.12 Statistical Analysis

Experimental data were processed and analyzed using GraphPad Prism 19.0 software (Dotmatics, Boston, MA, USA). Quantitative data are presented as mean $\pm$ standard deviation (SD) from at least three independent experiments. Statistical comparisons between groups were conducted using one-way analysis of variance (ANOVA) followed by Tukey's post-hoc test for multiple comparisons. For two-group comparisons, an unpaired two-tailed Student's *t*-test was applied. *p*-values less than 0.05 were considered statistically significant. Kaplan-Meier survival curves were analyzed using the log-rank (Mantel-Cox) test. Correlation analysis was performed using Pearson's correlation coefficient. All figures were generated with GraphPad Prism, and results were interpreted in the context of their biological relevance.

3. Result

3.1 Bioinformatics Analysis Revealed Prominent Expression of PLIN3 in LUAD and its Strong Correlation with LUAD Prognosis

Querying the TCGA database *via* GEPIA (http://gepia2.cancer-pku.cn/#survival) and performing survival analysis using the Kaplan-Meier Plotter database confirmed

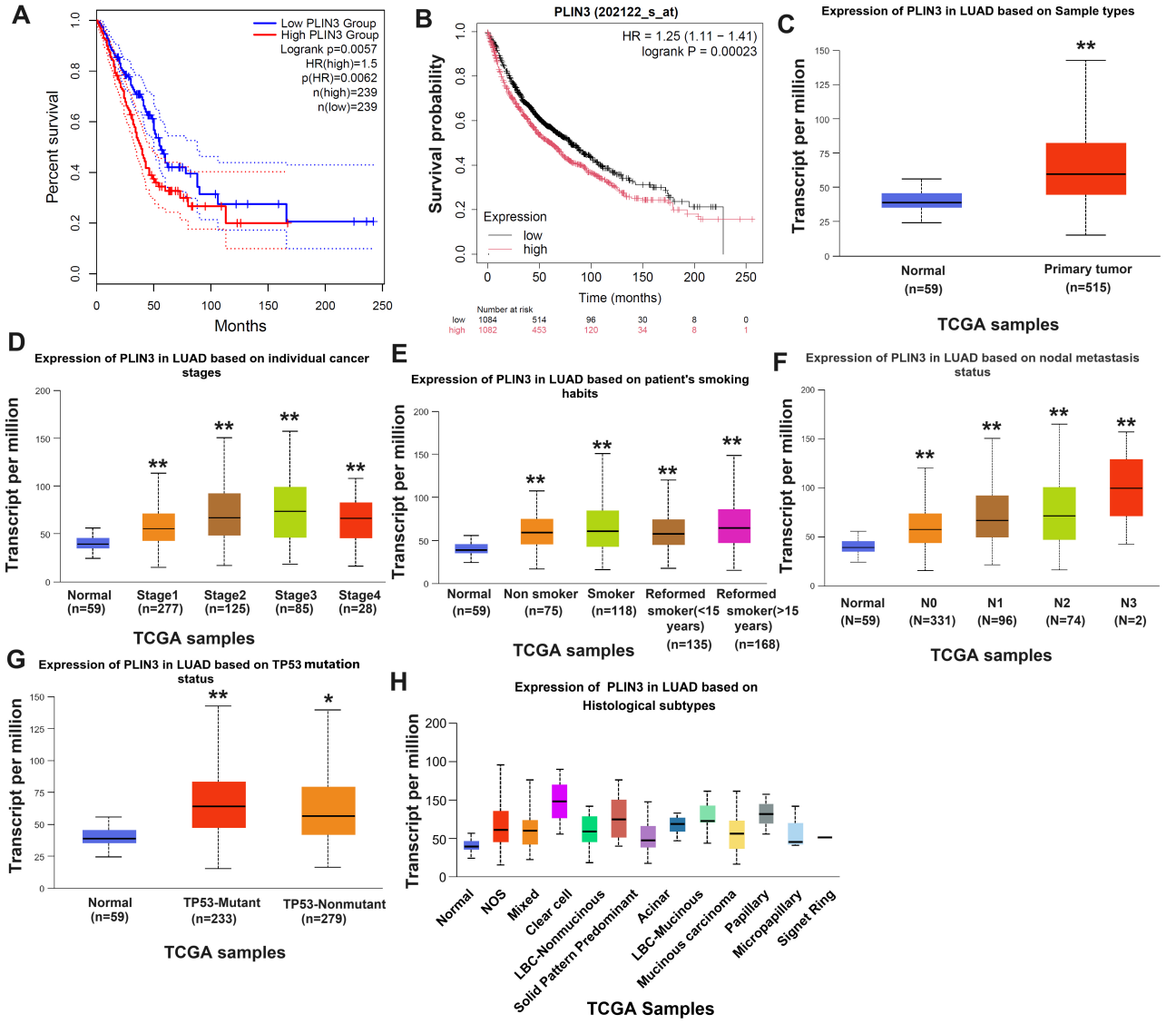

Fig. 1. Bioinformatics analysis revealed prominent expression of PLIN3 in LUAD and its strong correlation with LUAD prognosis. (A) Survival probabilities from the TCGA database *via* GEPIA (http://gepia2.cancer-pku.cn/#survival) for patients with LUAD exhibiting high (n = 239) and low/medium (n = 239) *PLIN3* expression ($p < 0.01$). (B) Survival probabilities from the Kaplan-Meier Plotter database for patients with LUAD exhibiting high (n = 1082) and low (n = 1084) *PLIN3* expression ($p = 0.00023$). *PLIN3* expression in LUAD across various sample types (C), cancer stages (D), smoking habits (E), nodal metastasis status (F), TP53 mutation status (G), and histological subtypes (H). *$p < 0.05$, **$p < 0.01$. PLIN3, perilipin 3; LUAD, lung adenocarcinoma; TCGA, the cancer genome atlas.

a strong association between elevated *PLIN3* expression and poor prognosis in LUAD (Fig. 1A,B). Results from both databases revealed that patients with higher *PLIN3* expression had significantly reduced survival times ($p < 0.0001$). Further analysis in the UALCAN database demonstrated that *PLIN3* is markedly upregulated in LUAD tissues (Fig. 1C), with consistent findings across various LUAD subgroups stratified by cancer stages, smoking history, nodal metastasis status, TP53 mutation status, and histological subtypes (Fig. 1D–H). *PLIN3* expression was significantly higher in all stages (1–4) compared to normal tissues ($p < 0.01$). Additionally, *PLIN3* expression was significantly higher in patients with LUAD regardless of smoking history compared to normal tissues ($p < 0.01$), suggesting that PLIN3 expression may be independent of smoking. Regarding nodal metastasis status, *PLIN3* expression levels were significantly elevated in patients across N0-N3 categories compared to normal ($p < 0.01$). For TP53 mutation status, both TP53-mutant and TP53-wildtype patients showed higher *PLIN3* expression compared to normal ($p < 0.01$). In summary, bioinformatics analyses provide compelling evidence that *PLIN3* is significantly upregulated in LUAD and is strongly associated with poor patient survival.

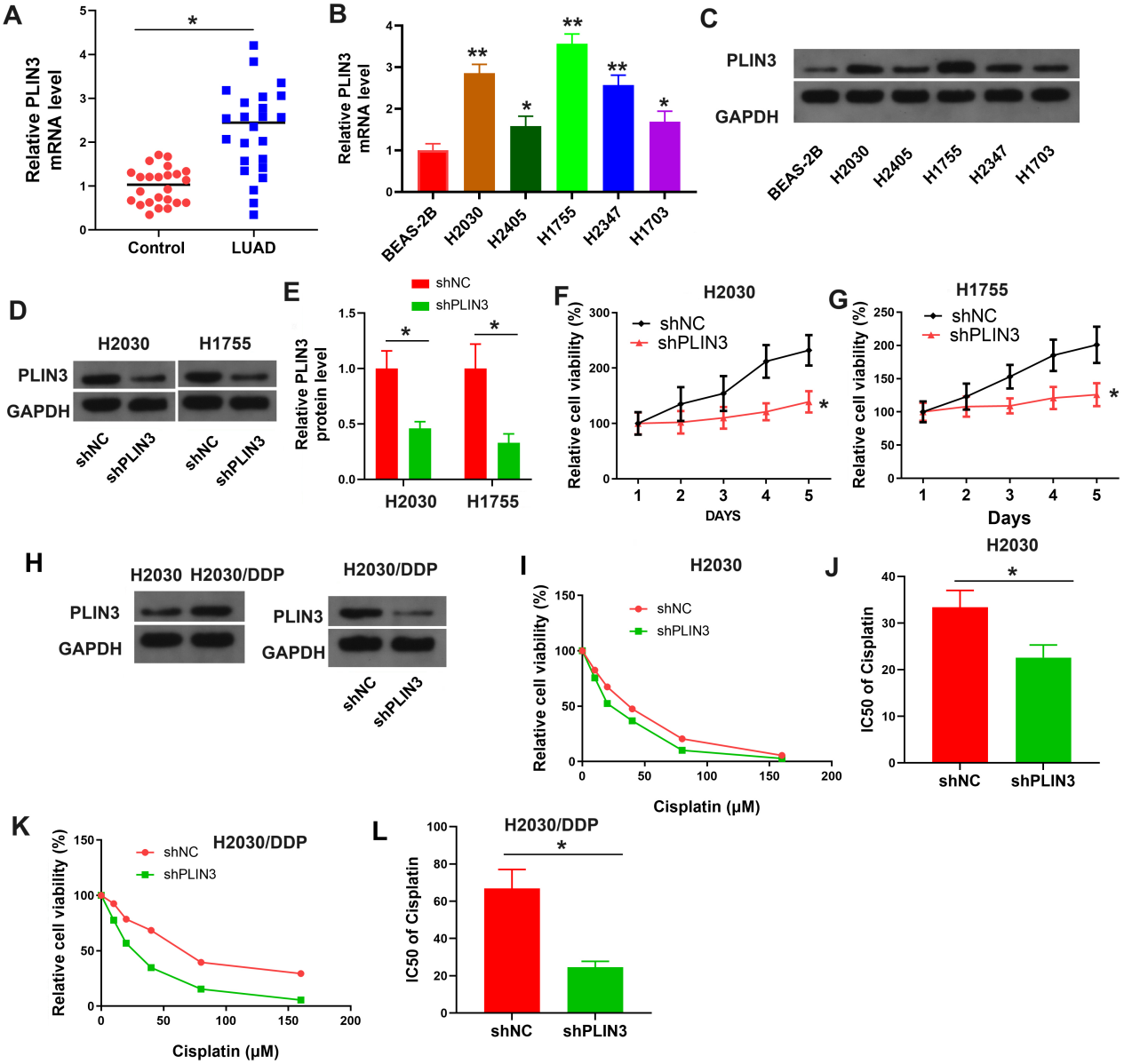

Fig. 2. *PLIN3* was markedly elevated in LUAD and promoted DDP resistance. (A) Relative *PLIN3* mRNA levels in normal and LUAD tissues (n = 24). Transcription (B) and translation (C) levels of *PLIN3* in five NSCLC cell lines. (D,E) Western blot analysis of PLIN3 translation levels in H2030 and H1775 cells transfected with shNC or sh*PLIN3*. Cell viability (F,G) of H2030 and H1775 cells transfected with shNC or sh*PLIN3*. (H) PLIN3 protein levels in H2030 and H2030/DDP cells (left) and in H2030/DDP cells transfected with shNC or sh*PLIN3* (right). Cell viability (I) and IC_{50} values (J) in gradient DDP concentrations of H2030 cells transfected with shNC or sh*PLIN3*. Cell viability (K) and IC_{50} values (L) in gradient DDP concentrations of H2030/DDP cells transfected with shNC or sh*PLIN3*. *$p < 0.05$, **$p < 0.01$. DDP, cisplatin; NSCLC, non-small cell lung cancer; shNC, short hairpin RNA negative control.

3.2 PLIN3 was Markedly Elevated in LUAD and Promoted DDP Resistance

Building on previous analyses, *PLIN3* mRNA levels were assessed in 24 pairs of normal and LUAD tissues, revealing a marked elevation in *PLIN3* expression in LUAD tissues (Fig. 2A). Consistent with these results, both transcriptional and translational levels of *PLIN3* were significantly upregulated in five NSCLC cell lines (H2030, H2405, H1755, H2347, and H1703) compared to normal BEAS-2B cells (Fig. 2B,C). Among these, *PLIN3* expression was most prominent in H2030 and H1775 cells, which were selected for further investigation. The impact of *PLIN3* knockdown was confirmed in H2030 and H1775 cells (Fig. 2D,E), with results showing that *PLIN3* knockdown notably reduced cell viability (Fig. 2F,G). In H2030/DDP cells, PLIN3 expression was significantly decreased compared to normal H2030 cells (Fig. 2H), and *PLIN3* shRNA also significantly reduced PLIN3 levels in

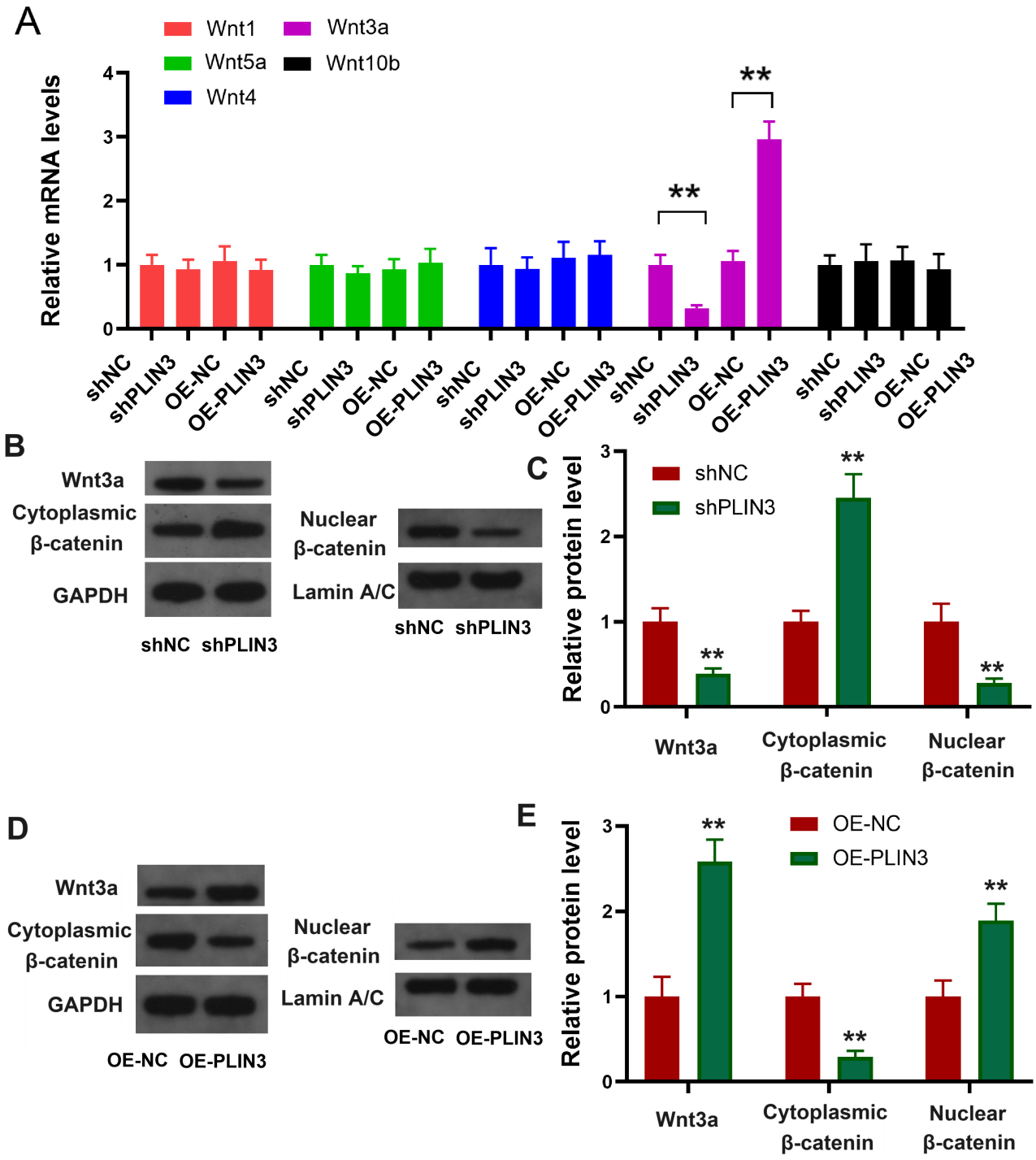

Fig. 3. PLIN3 activates the Wnt/β-catenin signaling pathway. (A) Relative mRNA levels of *Wnt* family members in DDP-resistant LUAD cells transfected with OE-*PLIN3* or sh*PLIN3*. Protein levels of Wnt3a, intracytoplasmic β-catenin, and nuclear β-catenin in DDP-resistant LUAD cells transfected with sh*PLIN3* (B,C) or OE-*PLIN3* (D,E). $^{**}p < 0.01$ compared to corresponding sh-NC or OE-NC groups. DDP, cisplatin; LUAD, lung Adenocarcinoma; OE, overexpressed; sh, short hairpin RNA.

H2030/DDP cells. Moreover, cytotoxicity assays demonstrated that PLIN3 shRNA treatment significantly increased the susceptibility of H2030 cells to DDP (Fig. 2I,J). The knockdown of *PLIN3* in H2030/DDP cells significantly diminished cell viability and reduced the IC_{50} value in response to DDP treatment (Fig. 2K,L). In conclusion, these results suggest that *PLIN3* is notably elevated in LUAD, playing a role in promoting DDP resistance.

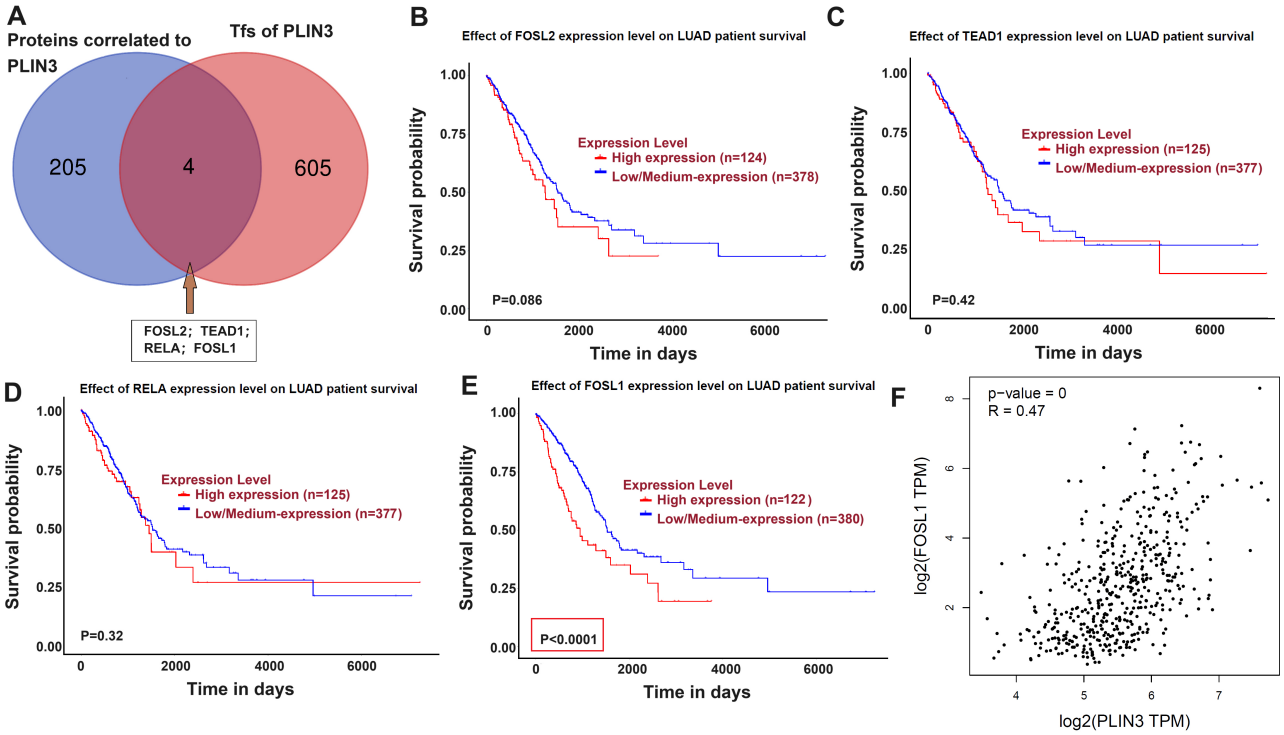

Fig. 4. FOSL1 may regulate PLIN3 expression. (A) Intersection of proteins correlated with *PLIN3* and transcription factors regulating *PLIN3*. Survival probabilities from the TCGA database for patients with LUAD exhibiting high or low/medium expression of FOSL2 (B), TEAD1 (C), RELA (D), and FOSL1 (E, $p < 0.0001$). (F) Positive linear correlation between *FOSL1* and *PLIN3* expression ($p = 0$, $R^2 = 0.47$). FOSL1, FOS-like antigen 1; FOSL2, FOS-like antigen 2; TEAD1, TEA domain transcription factor 1; RELA, v-rel avian reticuloendotheliosis viral oncogene homolog A.

3.3 PLIN3 Activates the Wnt/β-Catenin Signaling Pathway

Given the pivotal role of the Wnt/β-catenin signaling pathway in drug resistance mechanisms in lung cancer [25], DDP-resistant LUAD cells were subjected to either *PLIN3* overexpression or knockdown, and the impact on *Wnt* mRNA expression was subsequently assessed. Among the *Wnt* family members, only *Wnt3a* mRNA expression was significantly altered (Fig. 3A). To further validate these observations, the effects of *PLIN3* overexpression or knockdown on protein levels of intracytoplasmic Wnt3a, intracytoplasmic β-catenin, and nuclear β-catenin were evaluated. The results demonstrated that *PLIN3* knockdown notably reduced Wnt3a protein levels, increased intracytoplasmic β-catenin protein levels, and decreased nuclear β-catenin levels (Fig. 3B,C). Conversely, *PLIN3* overexpression induced the opposite effects (Fig. 3D,E). These results collectively indicate that *PLIN3* overexpression significantly upregulates *Wnt3a* expression, promotes β-catenin nuclear translocation, and activates the Wnt3a/β-catenin signaling pathway.

3.4 FOSL1 may Regulate PLIN3 Expression

To investigate the upstream regulatory factors of *PLIN3*, the TCGA database was queried to identify 205 proteins strongly correlated with *PLIN3* expression. The JASPAR database (https://jaspar.elixir.no/) was then used to identify 605 transcription factors (TFs) with potential binding sites in the *PLIN3* promoter region. The intersection of these two datasets revealed four common proteins: FOS-like antigen 2 (FOSL2), TEA domain transcription factor 1 (TEAD1), v-rel avian reticuloendotheliosis viral oncogene homolog A (RELA), and FOSL1 (Fig. 4A). Further analysis using the TCGA database evaluated the prognostic significance of these four proteins in patients with LUAD, revealing that only FOSL1 was consistently associated with poorer survival outcomes (Fig. 4B–E). Additionally, analysis from the GEPIA database (http://gepia.cancer-pku.cn/index.html) showed a positive linear correlation between *FOSL1* and *PLIN3* expression (Fig. 4F). These data suggest that FOSL1 may regulate *PLIN3* expression and influence survival in LUAD.

3.5 FOSL1 Promotes DDP Resistance in LUAD through Mediation of PLIN3

Building on previous findings regarding FOSL1's role in regulating *PLIN3* expression, its impact on DDP resistance in LUAD cells was further investigated. *FOSL1* translation and transcription levels were evaluated in normal lung cells and five NSCLC cell lines, with results revealing prominent *FOSL1* expression across all NSCLC

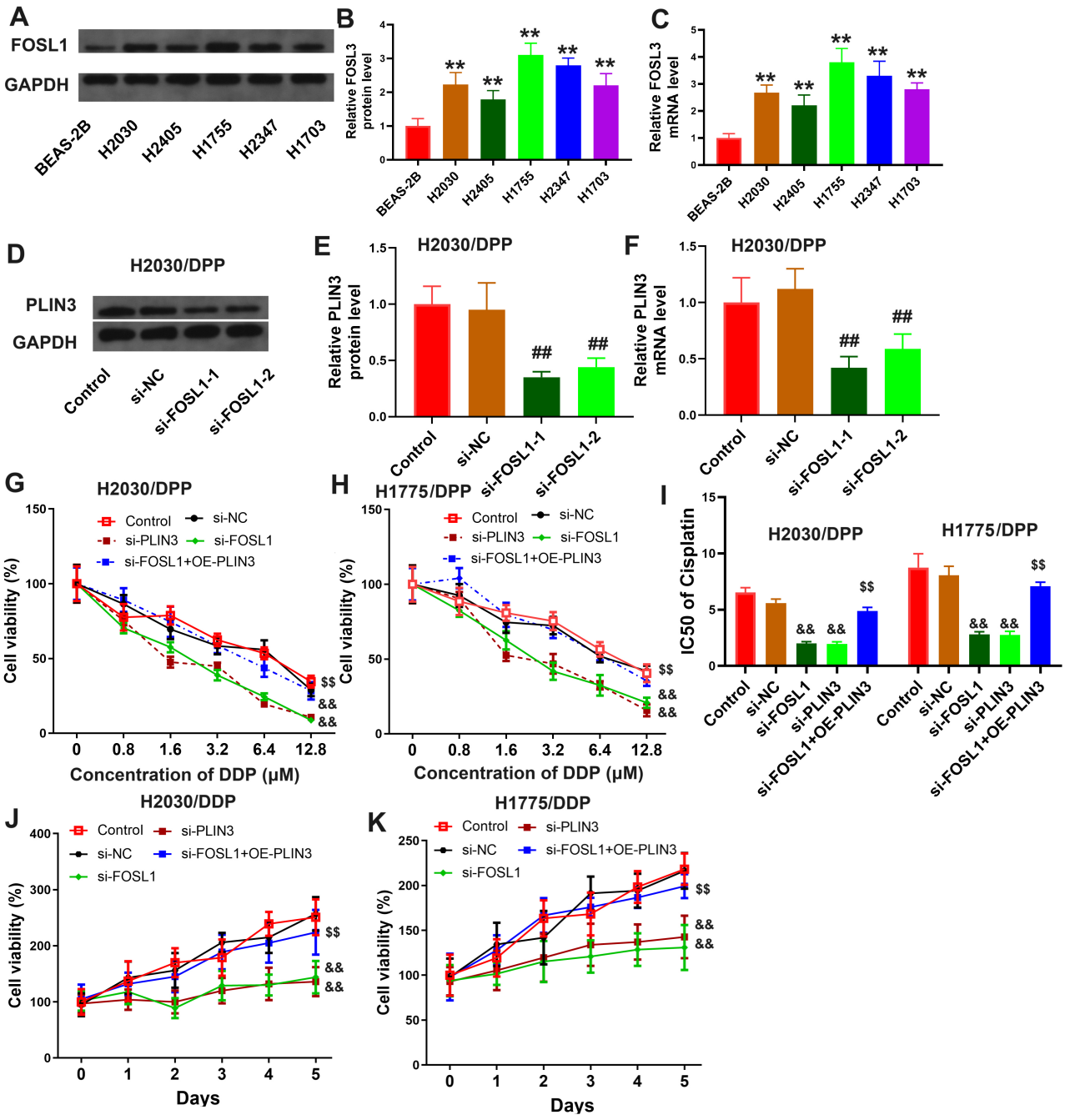

Fig. 5. FOSL1 promotes DDP resistance in LUAD through mediation of *PLIN3*. The translation (A,B) and transcription (C) levels of *FOSL1* in five NSCLC cell lines. The translation (D,E) and transcription (F) levels of *PLIN3* in H2030/DDP cells transfected with siNC or si*FOSL1*. The cell vitality (G,H) and IC_{50} values (I) in gradient DDP concentration of H2030/DDP and H1775/DDP cells treated with si*FOSL1*, si*PLIN3*, or si*FOSL1*+OE-*PLIN3*. (J,K) The cell vitality of H2030/DDP and H1755/DDP cells treated with si*FOSL1*, si*PLIN3*, or si*FOSL1*+OE-*PLIN3*. $^{**}p < 0.01$; $^{\#\#}p < 0.01$ compared to si-NC; $^{\&\&}p < 0.01$ compared to si-NC; $^{\$\$}p < 0.01$ compared to si-FOSL1.

cells (Fig. 5A–C). H2030/DDP cells were incubated with *FOSL1* siRNA, and the protein and mRNA levels of *PLIN3* were subsequently quantified. The results showed that both the transcriptional and translational levels of *PLIN3* were significantly reduced following *FOSL1* knockdown (Fig. 5D–F). Additionally, H2030/DDP and H1775/DDP cells were transfected with si*FOSL1*, si*PLIN3*, or a combination of si*FOSL1* and a *PLIN3* overexpression plasmid (si*FOSL1*+OE-*PLIN3*), and changes in cell viability and IC_{50} values at varying DDP concentrations were monitored. *FOSL1* and *PLIN3* knockdown increased the susceptibility of both H2030/DDP and H1775/DDP cells to DDP, while *PLIN3* overexpression mitigated the effects of *FOSL1* knockdown (Fig. 5G–I). Further survival as-

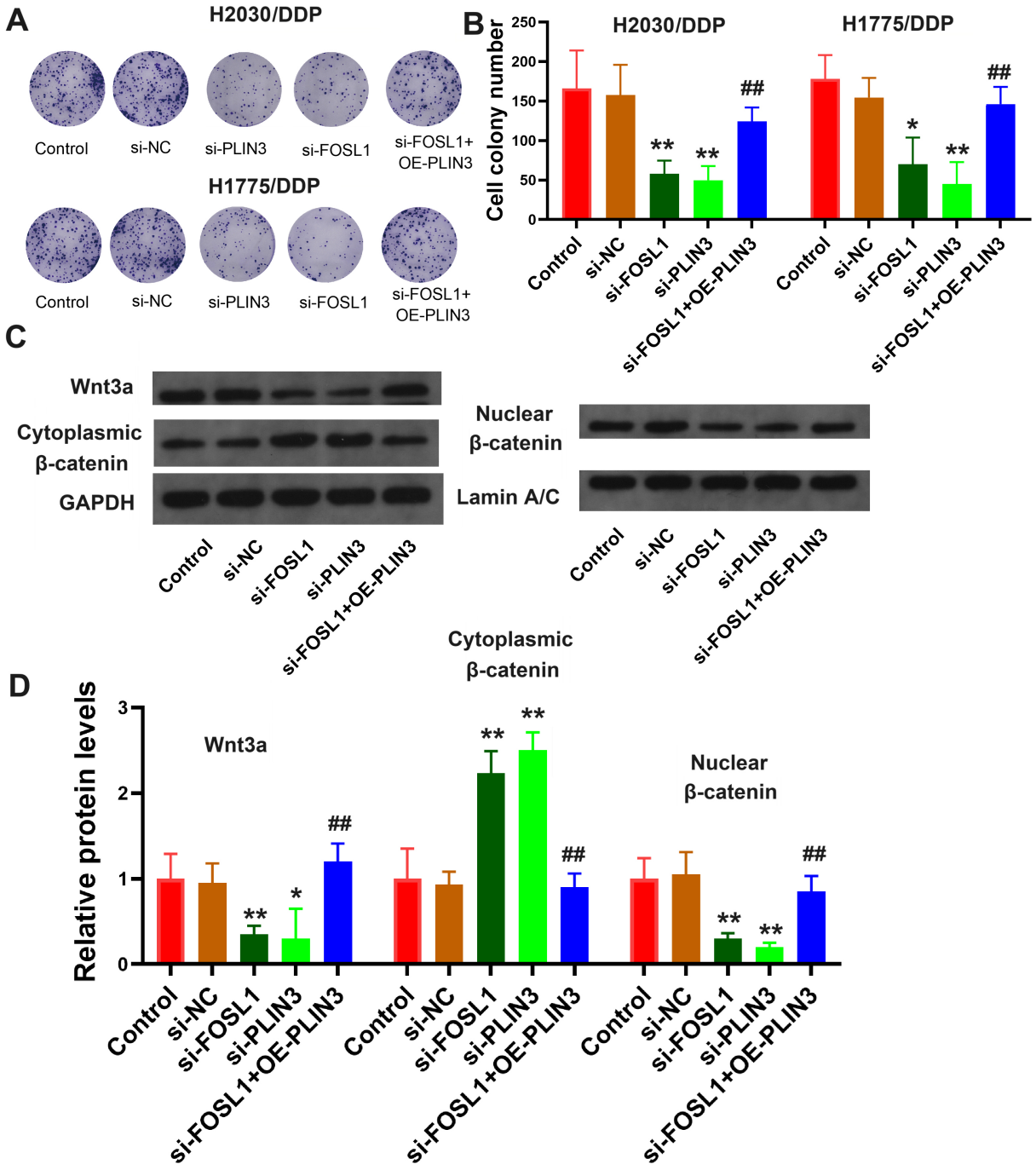

Fig. 6. FOSL1 enhances the clonogenic potential of DDP-resistant LUAD cells by triggering the Wnt3a/β-catenin signaling pathway *via* PLIN3. (A,B) The cell colony numbers of H2030/DDP and H1775/DDP cell lines treated with si*FOSL1*, si*PLIN3*, and si*FOSL1*+OE-*PLIN3*. (C,D) The protein levels of Wnt3a, intracytoplasmic β-catenin, and nuclear β-catenin in DDP-resistant LUAD cells treated with si*FOSL1*, si*PLIN3*, and si*FOSL1*+OE-*PLIN3*. *$p < 0.05$, **$p < 0.01$; $^{\#\#}p < 0.01$ compared to si-FOSL1.

sessments revealed that si*FOSL1* and si*PLIN3* treatments significantly impaired cell viability, whereas PLIN3 overexpression counteracted the detrimental effects of *FOSL1* knockdown on cell survival (Fig. 5J,K). These results highlight the role of FOSL1 in promoting DDP resistance in LUAD cells through the regulation of *PLIN3*.

3.6 FOSL1 Enhances the Clonogenic Potential of DDP-Resistant LUAD Cells by Triggering the Wnt3a/β-Catenin Signaling Pathway via PLIN3

DDP-resistant LUAD cell lines were treated with si*FOSL1*, si*PLIN3*, or si*FOSL1*+OE-*PLIN3*, and the number of cell clones, along with protein levels of Wnt3a, intracytoplasmic β-catenin, and nuclear β-catenin, were as-

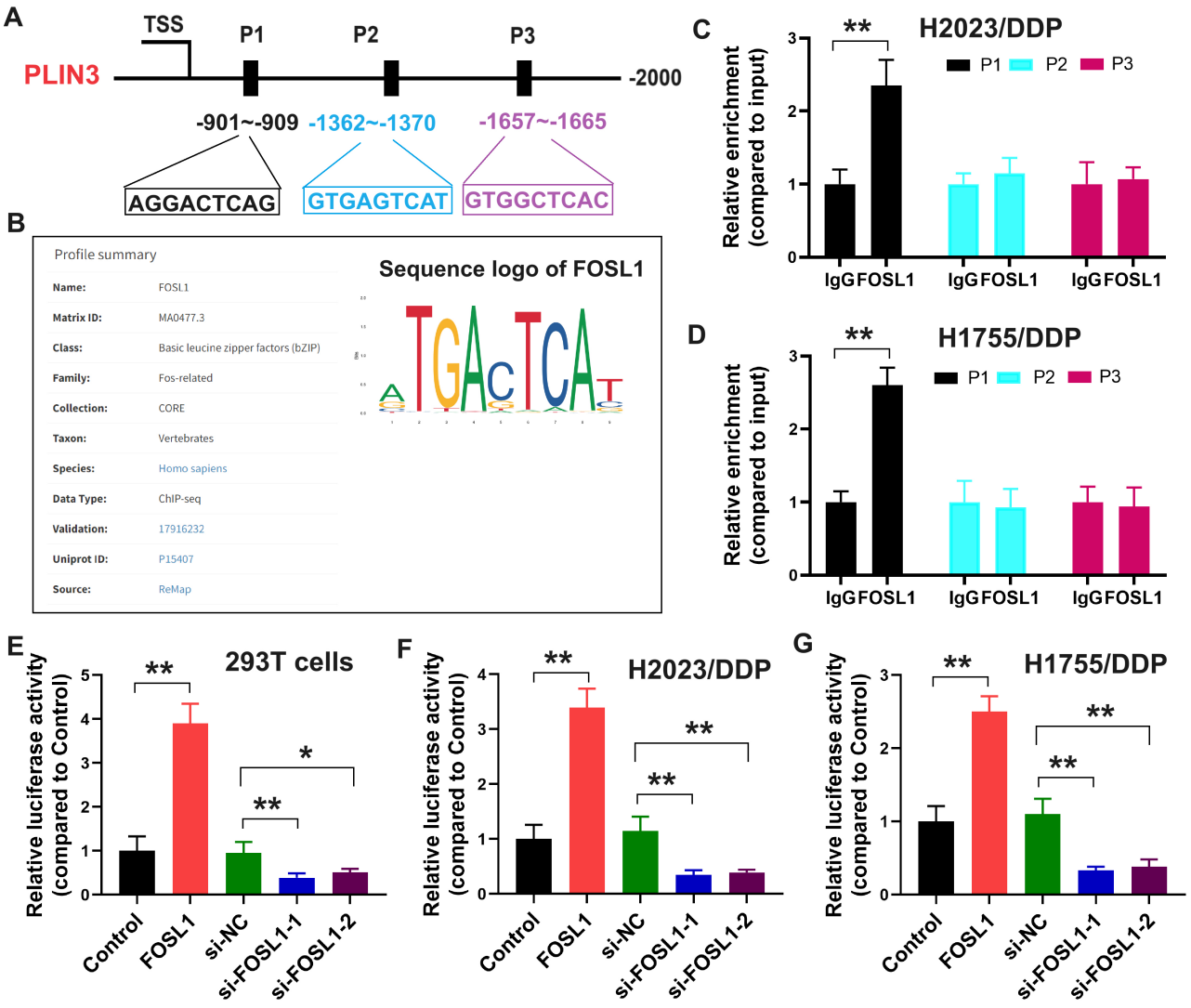

Fig. 7. The transcription factor FOSL1 promotes *PLIN3* expression *via* direct binding to the P1 sequence of the *PLIN3* promoter. (A) The potential binding sequences of FOSL1 to the *PLIN3* promoter identified by the JASPER database. (B) The profile summary and sequence logo of FOSL1 from the JASPER database. (C,D) The validation of the potential binding sequences of FOSL1 to the *PLIN3* promoter by chromatin immunoprecipitation assay in two cell lines. Luciferase reporter assays of *PLIN3* transcriptional activity following *FOSL1* overexpression and knockdown in 293T (E), H2030/DDP (F), and H1775/DDP (G) cells. *$p < 0.05$, **$p < 0.01$.

sessed. Results demonstrated that knockdown of *FOSL1* and *PLIN3* significantly reduced the number of cell clones (Fig. 6A,B) and lowered the levels of Wnt3a and nuclear β-catenin, while increasing cytoplasmic β-catenin levels (Fig. 6C,D). Conversely, *PLIN3* overexpression reversed the effects of *FOSL1* knockdown. These results suggest that FOSL1 promotes the Wnt3a/β-catenin signaling cascade by enhancing *Wnt3a* expression and facilitating β-catenin nuclear translocation through PLIN3.

3.7 The Transcription Factor FOSL1 Promotes PLIN3 Expression via Direct Binding to the P1 Sequence of the PLIN3 Promoter

To further investigate the sequence sites through which FOSL1 regulates *PLIN3* expression, a search of the JASPER database identified three potential binding sites of FOSL1 on the *PLIN3* promoter (P1-P3, Fig. 7A). The profile summary and sequence logo for FOSL1 were retrieved from the JASPER database (Fig. 7B). Chromatin immunoprecipitation (ChIP) assays confirmed that FOSL1 directly binds to the P1 sequence of the *PLIN3* promoter in DDP-resistant cells (Fig. 7C,D). Furthermore, luciferase reporter assays performed in 293T, H2030/DDP, and H1775/DDP cells revealed a significant increase in *PLIN3* promoter-driven reporter activity upon *FOSL1* overexpression and a marked decrease following *FOSL1* knockdown (Fig. 7E–G). These results indicate that FOSL1 enhances *PLIN3* expression by directly binding to the P1 sequence of the *PLIN3* promoter.

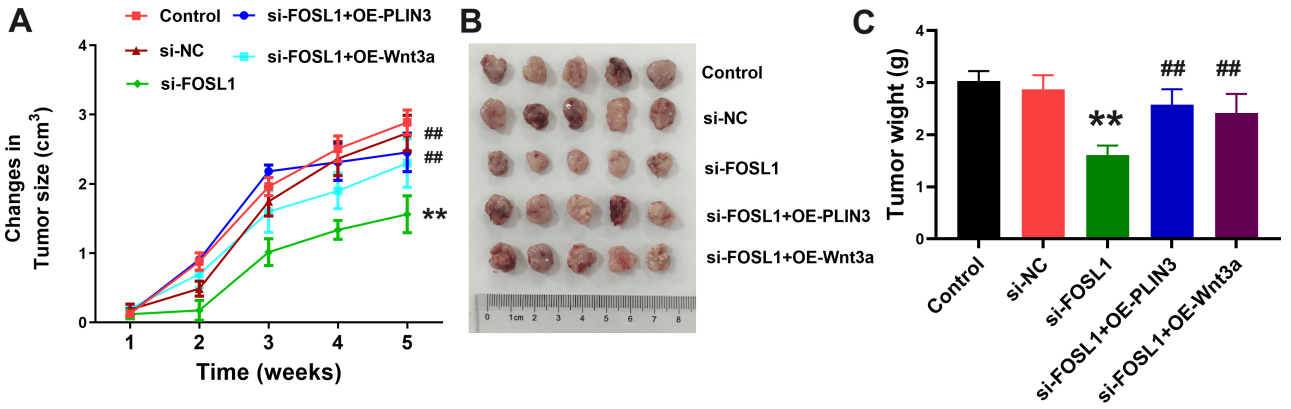

Fig. 8. Validation of FOSL1, PLIN3, and Wnt3a in mediating LUAD DDP resistance *in vivo*. (A,B) The growth rate of subcutaneous tumors following intraperitoneal administration of DDP in nude mice. (C) The weight of subcutaneous tumors following intraperitoneal administration of DDP in nude mice. $^{**}p < 0.01$; $^{\#\#}p < 0.01$ compared to si-FOSL1.

3.8 Validation of FOSL1, PLIN3, and Wnt3a in Mediating LUAD DDP Resistance in vivo Models

To assess the *in vivo* impact, H2030/DDP cells were treated with *FOSL1* siRNA in combination with *PLIN3* or *Wnt3a* overexpression plasmids (OE-*PLIN3* or OE-*Wnt3a*) and subcutaneously implanted into nude mice. Tumor growth was monitored following intraperitoneal administration of DDP (2 mg/kg) twice a week. The results showed that *FOSL1* knockdown significantly suppressed tumor growth and weight in the subcutaneous model, whereas overexpression of *PLIN3* or *Wnt3a* reversed this effect (Fig. 8A–C). These *in vivo* data confirm that FOSL1 promotes DDP resistance in LUAD through upregulation of *PLIN3* and *Wnt3a*.

4. Discussion

LUAD, the most prevalent subtype of lung cancer, presents significant diagnostic challenges due to its often asymptomatic early stages, which contribute to delayed detection and poor prognosis [2,26–29]. At advanced stages, systemic therapies, including chemotherapy, remain the primary treatment options [29–32]. DDP-based chemotherapy is a cornerstone of LUAD management [33,34], with initial responses typically promising; however, the eventual development of resistance significantly limits its long-term effectiveness [8,35]. Notably, DDP resistance is more pronounced in LUAD compared to LUSC [7,8], emphasizing the urgent need for a deeper understanding of the underlying biological mechanisms of DDP resistance to develop more effective therapeutic strategies.

One key factor implicated in cancer progression and chemoresistance is LD accumulation, commonly observed in cancer cells [10,16,36]. LDs, as the primary organelles responsible for storing neutral lipids in eukaryotic cells, play critical roles in cellular metabolism, membrane synthesis, and steroidogenesis [10,14–16]. Additionally, they are closely linked to various cancer-related processes, including tumorigenesis, invasion, metastasis, and chemoresistance [10,16]. PLIN3, located on the surface of LDs, is essential for LD formation, structural integrity, and functional regulation [37,38]. Overexpression of PLIN3 has been associated with poor prognosis in multiple cancers, including breast cancer, clear cell renal cell carcinoma, and hepatocellular carcinoma [18–20]. Our study demonstrates that PLIN3 is significantly upregulated in LUAD and that its overexpression correlates with unfavorable clinical outcomes. Notably, PLIN3 elevation is involved in the development of DDP resistance in LUAD, likely through the regulation of lipid metabolism, thereby supporting cancer cell survival under chemotherapy-induced stress.

The Wnt signaling pathway, a highly conserved system, regulates cell proliferation and differentiation, primarily by stabilizing cytoplasmic β-catenin, which then translocates to the nucleus to activate downstream genes [39]. Dysregulation of the Wnt/β-catenin pathway has been strongly associated with DDP resistance in lung cancer. For example, Ribonucleotide Reductase M2 has been shown to enhance DDP resistance in LUAD cells through activation of the Wnt/β-catenin signaling cascade [40]. Conversely, miR-32 and miR-548a inhibit the Wnt/β-catenin pathway by blocking Roundabout homolog 1, thus increasing DDP sensitivity in NSCLC cells [41]. Additionally, miR-448 modulates Wnt/β-catenin signaling by targeting special AT-rich sequence binding protein 1 (SATB1), thereby reversing DDP resistance in lung cancer cells [42]. As a member of the PLIN family, PLIN2 has been shown to promote tumor growth by modulating GSK3 and Wnt/β-catenin signaling [43]. Building on this, it was hypothesized that PLIN3 may also play a role in the Wnt signaling pathway. Consistent with this hypothesis, our findings indicate that PLIN3 significantly enhances Wnt3a expression and facilitates β-catenin nuclear translocation, thereby contributing to DDP resistance in LUAD. This discovery highlights a previously

unrecognized link between PLIN3 and the Wnt signaling pathway in mediating chemoresistance.

This study identifies FOSL1 as the sole transcription factor significantly associated with both PLIN3 expression and reduced survival in patients with LUAD. FOSL1, a subunit of the AP-1 transcription factor complex, plays a critical role in cell differentiation, stress response, and tumorigenesis [44]. Previous research has demonstrated that FOSL1 is pivotal in the progression of lung cancer, particularly in KRAS-mutant variants, where its elevated expression correlates with poor prognosis [45]. Mechanistically, FOSL1 promotes KRAS-driven lung cancer by regulating survival genes and amphiregulin expression [46]. However, its role in tumor drug resistance has remained largely unexplored. In this study, the direct interaction between FOSL1 and the PLIN3 promoter was further confirmed. A combination of *in vitro* and *in vivo* experiments demonstrated that FOSL1 regulates PLIN3 transcription, subsequently activating the Wnt3a/β-catenin pathway and promoting DDP resistance in LUAD. These findings provide novel insights into the involvement of FOSL1 in tumor DDP resistance, offering a potential therapeutic target for overcoming DDP resistance in LUAD.

Several limitations of this study should be acknowledged. First, the reliance on bioinformatics databases for analyzing PLIN3 expression and its correlation with patient prognosis may introduce potential bias or inaccuracies. Second, the use of *in vitro* cell line models to investigate the mechanisms of PLIN3 in DDP resistance may not fully capture the complexity of tumor biology in patient tissues. Third, the findings are primarily based on experiments conducted in cell lines, which may not accurately represent the *in vivo* tumor microenvironment. The effects of PLIN3, FOSL1, and Wnt3a/β-catenin signaling on DDP resistance may be influenced by factors present in the tumor microenvironment, which are not reflected in cell culture models.

5. Conclusion

In conclusion, this study establishes that PLIN3 promotes DDP resistance in LUAD by stimulating the Wnt3a/β-catenin signaling pathway. FOSL1 was identified as a central TF that directly regulates PLIN3 expression, enhancing DDP resistance. Future research should focus on developing inhibitors targeting the FOSL1/PLIN3/Wnt/β-catenin axis, with the aim of their clinical application in LUAD.

Availability of Data and Materials

The data supporting our results are available from the GEPIA database (http://gepia2.cancer-pku.cn/#survival), Kaplan-Meier Plotter database (https://kmplot.com/analysis/) and the UALCAN database (https://ualcan.path.uab.edu/) and from the corresponding author upon reasonable request.

Author Contributions

WNT: Conceptualization, Investigation, Writing—original draft, and Data curation; JJS: Conceptualization and Investigation; HBW: Conceptualization, Investigation, Resources; YHH: Investigation, Visualization, Validation; CXW: Data curation; MR: Methodology; JL: Methodology; DLX: Validation; JGD: Data curation; HW: Formal analysis, Visualization; DMZ: Formal analysis; BS: Resources, Validation; ZGC: Conceptualization, Project administration, Supervision, and Writing—review & editing. All authors contributed to editorial changes in the manuscript. All authors read and approved the final manuscript. All authors have participated sufficiently in the work and agreed to be accountable for all aspects of the work.

Ethics Approval and Consent to Participate

The animal procedures were approved by the Animal Ethics Committee of the PLA Navy Medical Center (Approval number AF-HEC-069), adhered to the Animal Research: Reporting of *In Vivo* Experiments (ARRIVE) guidelines 2019. The clinical study involving human participants was approved by the Ethics Committee of the PLA Navy Medical Center (Approval number AF-HEC-068), and all patients or their families/legal guardians provided written informed consent. The study was carried out in accordance with the guidelines of the Declaration of Helsinki.

Acknowledgment

Not applicable.

Funding

This research received no external funding.

Conflict of Interest

The authors declare no conflict of interest.

Declaration of AI and AI-Assisted Technologies in the Writing Process

During the preparation of this work, the authors used ERNIE Bot to check spelling and grammar (mainly Discussion section). After using this tool, the authors reviewed and edited the content as needed and take full responsibility for the content of the publication.

Supplementary Material

Supplementary material associated with this article can be found, in the online version, at https://doi.org/10.31083/FBL26898.

References

[1] Bray F, Laversanne M, Sung H, Ferlay J, Siegel RL, Soerjomataram I, *et al*. Global cancer statistics 2022: GLOBOCAN estimates of incidence and mortality worldwide for 36 cancers

in 185 countries. CA: a Cancer Journal for Clinicians. 2024; 74: 229–263. https://doi.org/10.3322/caac.21834.

[2] Zhang Y, Vaccarella S, Morgan E, Li M, Etxeberria J, Chokunonga E, *et al*. Global variations in lung cancer incidence by histological subtype in 2020: a population-based study. The Lancet. Oncology. 2023; 24: 1206–1218. https://doi.org/10.1016/S1470-2045(23)00444-8.

[3] Heigener DF, Kerr KM, Laing GM, Mok TSK, Moiseyenko FV, Reck M. Redefining Treatment Paradigms in First-line Advanced Non-Small-Cell Lung Cancer. Clinical Cancer Research. 2019; 25: 4881–4887. https://doi.org/10.1158/1078-0432.CCR-18-1894.

[4] Cui J, He Y, Zhu F, Gong W, Zuo R, Wang Y, *et al*. Inetetamab, a novel anti-HER2 monoclonal antibody, exhibits potent synergistic anticancer effects with cisplatin by inducing pyroptosis in lung adenocarcinoma. International Journal of Biological Sciences. 2023; 19: 4061–4081. https://doi.org/10.7150/ijbs.82980.

[5] El-Hussein A, Manoto SL, Ombinda-Lemboumba S, Alrowaili ZA, Mthunzi-Kufa P. A Review of Chemotherapy and Photodynamic Therapy for Lung Cancer Treatment. Anti-cancer Agents in Medicinal Chemistry. 2021; 21: 149–161. https://doi.org/10.2174/1871520620666200403144945.

[6] Li R, Liu J, Fang Z, Liang Z, Chen X. Identification of Mutations Related to Cisplatin-Resistance and Prognosis of Patients With Lung Adenocarcinoma. Frontiers in Pharmacology. 2020; 11: 572627. https://doi.org/10.3389/fphar.2020.572627.

[7] Cui Z, Zhang L, Song L. Differences of inflammatory microenvironment and sensitive correlation to cisplatin-chemotherapy in lung adenocarcinoma and squamous cell carcinoma. STEMedicine. 2022; 3: e151–e151.

[8] Kryczka J, Kryczka J, Czarnecka-Chrebelska KH, Brzeziańska-Lasota E. Molecular Mechanisms of Chemoresistance Induced by Cisplatin in NSCLC Cancer Therapy. International Journal of Molecular Sciences. 2021; 22: 8885. https://doi.org/10.3390/ijms22168885.

[9] Lamprou I, Tsolou A, Kakouratos C, Mitrakas AG, Xanthopoulou ET, Kassela K, *et al*. Suppressed PLIN3 frequently occurs in prostate cancer, promoting docetaxel resistance via intensified autophagy, an event reversed by chloroquine. Medical Oncology. 2021; 38: 116. https://doi.org/10.1007/s12032-021-01566-y.

[10] Cruz ALS, Barreto EDA, Fazolini NPB, Viola JPB, Bozza PT. Lipid droplets: platforms with multiple functions in cancer hallmarks. Cell Death & Disease. 2020; 11: 105. https://doi.org/10.1038/s41419-020-2297-3.

[11] Beloribi-Djefaflia S, Vasseur S, Guillaumond F. Lipid metabolic reprogramming in cancer cells. Oncogenesis. 2016; 5: e189. https://doi.org/10.1038/oncsis.2015.49.

[12] Lei Y, Zhou B, Meng X, Liang M, Song W, Liang Y, *et al*. A risk score model based on lipid metabolism-related genes could predict response to immunotherapy and prognosis of lung adenocarcinoma: a multi-dataset study and cytological validation. Discover Oncology. 2023; 14: 188. https://doi.org/10.1007/s12672-023-00802-3.

[13] Liang L, He H, Jiang S, Liu Y, Huang J, Sun X, *et al*. *TIAM2* Contributes to Osimertinib Resistance, Cell Motility, and Tumor-Associated Macrophage M2-like Polarization in Lung Adenocarcinoma. International Journal of Molecular Sciences. 2022; 23: 10415. https://doi.org/10.3390/ijms231810415.

[14] Thiele C, Spandl J. Cell biology of lipid droplets. Current Opinion in Cell Biology. 2008; 20: 378–385. https://doi.org/10.1016/j.ceb.2008.05.009.

[15] Martin S, Parton RG. Lipid droplets: a unified view of a dynamic organelle. Nature Reviews. Molecular Cell Biology. 2006; 7: 373–378. https://doi.org/10.1038/nrm1912.

[16] Royo-García A, Courtois S, Parejo-Alonso B, Espiau-Romera P, Sancho P. Lipid droplets as metabolic determinants for stemness and chemoresistance in cancer. World Journal of Stem Cells. 2021; 13: 1307–1317. https://doi.org/10.4252/wjsc.v13.i9.1307.

[17] Greenberg AS, Egan JJ, Wek SA, Garty NB, Blanchette-Mackie EJ, Londos C. Perilipin, a major hormonally regulated adipocyte-specific phosphoprotein associated with the periphery of lipid storage droplets. The Journal of Biological Chemistry. 1991; 266: 11341–11346.

[18] Zhang X, Su L, Sun K. Expression status and prognostic value of the perilipin family of genes in breast cancer. American Journal of Translational Research. 2021; 13: 4450–4463.

[19] Wang K, Ruan H, Song Z, Cao Q, Bao L, Liu D, *et al*. PLIN3 is up-regulated and correlates with poor prognosis in clear cell renal cell carcinoma. Urologic Oncology. 2018; 36: 343.e9–343.e19. https://doi.org/10.1016/j.urolonc.2018.04.006.

[20] Zhang Y, Liang X, Lian Q, Liu L, Zhang B, Dong Z, *et al*. Transcriptional analysis of the expression and prognostic value of lipid droplet-localized proteins in hepatocellular carcinoma. BMC Cancer. 2023; 23: 677. https://doi.org/10.1186/s12885-023-10987-z.

[21] Wu YJ, Wang J, Zhang P, Yuan LX, Ju LL, Wang HX, *et al*. PIWIL1 interacting RNA piR-017724 inhibits proliferation, invasion, and migration, and inhibits the development of HCC by silencing PLIN3. Frontiers in Oncology. 2023; 13: 1203821. https://doi.org/10.3389/fonc.2023.1203821.

[22] Lung J, Hung MS, Wang TY, Chen KL, Luo CW, Jiang YY, *et al*. Lipid Droplets in Lung Cancers Are Crucial for the Cell Growth and Starvation Survival. International Journal of Molecular Sciences. 2022; 23: 12533. https://doi.org/10.3390/ijms232012533.

[23] Men X, Zhu W. Silencing of Perilipin 3 Inhibits Lung Adenocarcinoma Cell Immune Resistance by Regulating the Transcription of PD-L1 Through c-Myc. Immunological Investigations. 2023; 52: 815–831. https://doi.org/10.1080/08820139.2023.2244976.

[24] Sirois I, Aguilar-Mahecha A, Lafleur J, Fowler E, Vu V, Scriver M, *et al*. A Unique Morphological Phenotype in Chemoresistant Triple-Negative Breast Cancer Reveals Metabolic Reprogramming and PLIN4 Expression as a Molecular Vulnerability. Molecular Cancer Research. 2019; 17: 2492–2507. https://doi.org/10.1158/1541-7786.MCR-19-0264.

[25] Entezari M, Deldar Abad Paskeh M, Orouei S, Kakavand A, Rezaei S, Sadat Hejazi E, *et al*. Wnt/β-catenin Signaling in Lung Cancer: Association with Proliferation, Metastasis, and Therapy Resistance. Current Cancer Drug Targets. 2023. https://doi.org/10.2174/1568009623666230413094317 (online ahead of print)

[26] Ji X, Zhu R, Gao C, Xie H, Gong X, Luo J. Hypoxia-Derived Exosomes Promote Lung Adenocarcinoma by Regulating HS3ST1-GPC4-Mediated Glycolysis. Cancers. 2024; 16: 695. https://doi.org/10.3390/cancers16040695.

[27] Lian X, Cao D, Hu X, Mo W, Yao X, Mo J, *et al*. Circular RNAs Hsa_circ_101555 and Hsa_circ_008068 as Diagnostic Biomarkers for Early-Stage Lung Adenocarcinoma. International Journal of General Medicine. 2022; 15: 5579–5589. https://doi.org/10.2147/IJGM.S367999.

[28] Chen Q, Wang X, Hu J. Systematically integrative analysis identifies diagnostic and prognostic candidates and small-molecule drugs for lung adenocarcinoma. Translational Cancer Research. 2021; 10: 3619–3646. https://doi.org/10.21037/tcr-21-526.

[29] Chen Y, Jin L, Jiang Z, Liu S, Feng W. Identifying and Validating Potential Biomarkers of Early Stage Lung Adenocarcinoma Diagnosis and Prognosis. Frontiers in Oncology. 2021; 11: 644426. https://doi.org/10.3389/fonc.2021.644426.

[30] Chen P, Liu Y, Wen Y, Zhou C. Non-small cell lung cancer in

China. Cancer Communications. 2022; 42: 937–970. https://doi.org/10.1002/cac2.12359.
[31] Duma N, Santana-Davila R, Molina JR. Non-Small Cell Lung Cancer: Epidemiology, Screening, Diagnosis, and Treatment. Mayo Clinic Proceedings. 2019; 94: 1623–1640. https://doi.org/10.1016/j.mayocp.2019.01.013.
[32] Baudoux N, Friedlaender A, Addeo A. Evolving Therapeutic Scenario of Stage III Non-Small-Cell Lung Cancer. Clinical Medicine Insights. Oncology. 2023; 17: 11795549231152948. https://doi.org/10.1177/11795549231152948.
[33] Fennell DA, Summers Y, Cadranel J, Benepal T, Christoph DC, Lal R, *et al*. Cisplatin in the modern era: The backbone of first-line chemotherapy for non-small cell lung cancer. Cancer Treatment Reviews. 2016; 44: 42–50. https://doi.org/10.1016/j.ctrv.2016.01.003.
[34] Griesinger F, Korol EE, Kayaniyil S, Varol N, Ebner T, Goring SM. Efficacy and safety of first-line carboplatin-versus cisplatin-based chemotherapy for non-small cell lung cancer: A meta-analysis. Lung Cancer. 2019; 135: 196–204. https://doi.org/10.1016/j.lungcan.2019.07.010.
[35] Galluzzi L, Senovilla L, Vitale I, Michels J, Martins I, Kepp O, *et al*. Molecular mechanisms of cisplatin resistance. Oncogene. 2012; 31: 1869–1883. https://doi.org/10.1038/onc.2011.384.
[36] APFFEL CA, BAKER JR. LIPID DROPLETS IN THE CYTOPLASM OF MALIGNANT CELLS. Cancer. 1964; 17: 176–184. https://doi.org/10.1002/1097-0142(196402)17:2<176::aid-cncr2820170207>3.0.co;2-2.
[37] Straub BK, Herpel E, Singer S, Zimbelmann R, Breuhahn K, Macher-Goeppinger S, *et al*. Lipid droplet-associated PAT-proteins show frequent and differential expression in neoplastic steatogenesis. Modern Pathology. 2010; 23: 480–492. https://doi.org/10.1038/modpathol.2009.191.
[38] Kimmel AR, Brasaemle DL, McAndrews-Hill M, Sztalryd C, Londos C. Adoption of PERILIPIN as a unifying nomenclature for the mammalian PAT-family of intracellular lipid storage droplet proteins. Journal of Lipid Research. 2010; 51: 468–471. https://doi.org/10.1194/jlr.R000034.
[39] Steinhart Z, Angers S. Wnt signaling in development and tissue homeostasis. Development. 2018; 145: dev146589. https://doi.org/10.1242/dev.146589.
[40] Jiang Y, Hu X, Pang M, Huang Y, Ren B, He L, *et al*. RRM2 mediated Wnt/β catenin signaling pathway activation in lung adenocarcinoma: A potential prognostic biomarker. Oncology Letters. 2023; 26: 417. https://doi.org/10.3892/ol.2023.14003.
[41] Zheng J, Li X, Cai C, Hong C, Zhang B. MicroRNA-32 and MicroRNA-548a Promote the Drug Sensitivity of Non-Small Cell Lung Cancer Cells to Cisplatin by Targeting ROBO1 and Inhibiting the Activation of Wnt/β-Catenin Axis. Cancer Management and Research. 2021; 13: 3005–3016. https://doi.org/10.2147/CMAR.S295003.
[42] Ning MY, Cheng ZL, Zhao J. MicroRNA-448 targets SATB1 to reverse the cisplatin resistance in lung cancer via mediating Wnt/β-catenin signalling pathway. Journal of Biochemistry. 2020; 168: 41–51. https://doi.org/10.1093/jb/mvaa024.
[43] Sun C, Luan S, Zhang G, Wang N, Shao H, Luan C. CEBPA-mediated upregulation of the lncRNA PLIN2 promotes the development of chronic myelogenous leukemia via the GSK3 and Wnt/β-catenin signaling pathways. American Journal of Cancer Research. 2017; 7: 1054–1067.
[44] Sobolev VV, Khashukoeva AZ, Evina OE, Geppe NA, Chebysheva SN, Korsunskaya IM, *et al*. Role of the Transcription Factor FOSL1 in Organ Development and Tumorigenesis. International Journal of Molecular Sciences. 2022; 23: 1521. https://doi.org/10.3390/ijms23031521.
[45] Vallejo A, Perurena N, Guruceaga E, Mazur PK, Martinez-Canarias S, Zandueta C, *et al*. An integrative approach unveils FOSL1 as an oncogene vulnerability in KRAS-driven lung and pancreatic cancer. Nature Communications. 2017; 8: 14294. https://doi.org/10.1038/ncomms14294.
[46] Elangovan IM, Vaz M, Tamatam CR, Potteti HR, Reddy NM, Reddy SP. FOSL1 Promotes Kras-induced Lung Cancer through Amphiregulin and Cell Survival Gene Regulation. American Journal of Respiratory Cell and Molecular Biology. 2018; 58: 625–635. https://doi.org/10.1165/rcmb.2017-0164OC.